P6.30 CLIMATE DATA RECORDS FROM MERGED CERES AND GEOSTATIONARY IMAGER DATA

David F. Young, Bruce A. Wielicki, Takmeng Wong, Lin H.. Chambers
NASA Langley Research Center, Hampton, VA

David R. Doelling, Dennis F. Keyes
AS&M, Inc., Hampton, VA

1. INTRODUCTION

Stable climate data records from satellite-based instruments are required for the detection of subtle climate trends. Changes in availability of data, orbital characteristics, sampling patterns, and calibration can all cause spurious trends in climate records derived from space-based instruments. Greater stability in climate data records can be achieved by incorporating the varying strengths of multiple satellite-based instruments in different orbits. The operational products from the Clouds in the Earth's Radiant Energy System (CERES) experiment are assimilating data from up to 8 separate spacecraft in order to produce the most accurate radiation budget data set to date. CERES has measured shortwave (SW: 0.3 – 5.0 μm) and longwave (LW: 5.0 – 200. μm) broadband radiance from five instruments on three spacecraft (Wielicki et al., 1996). The four instruments aboard The Terra and Aqua spacecraft are currently operating nominally with calibration accuracy of better than 1% in the SW and 0.5% in the LW with calibration stability of 0.1%/year. CERES has also greatly increased the accuracy the estimates on instantaneous flux from the radiance measurements via the production of improved angular distribution models (ADM) (Loeb et al., 2003a and 2003b).

One area where the CERES climate record can be further improved through the use of additional data from other satellites is in the removal of temporal sampling errors. Low Earth orbit (LEO) satellites such as Terra and Aqua cannot adequately define the diurnal cycle of radiation. Estimates of monthly mean flux based on a single sun-synchronous satellite can be biased by more than 20 W/m^2 in climatic regions with pronounced diurnal cycles. Instruments aboard geostationary (GEO) satellites have the capability of viewing regions during the complete diurnal cycle. Unfortunately, except for the recently launched Geostationary Earth Radiation Budget Instrument (GERB), there are no well-calibrated broadband measurements available from GEO. Narrowband GEO data can be merged with CERES data to remove temporal sampling errors as long as careful consideration is given to calibration, spectral differences, and proper use of broadband ADM with narrowband data (Young et al., 1998; Viollier et al., 2004; Standfuss et al., 2001). Particular emphasis must be given to using the well-calibrated CERES observations as the absolute calibration source, and using the GEO data to provide information concerning diurnal variability. The GEO data provide the definition of the magnitude of the diurnal variability but the estimates of hourly top of the atmosphere (TOA) fluxes are normalized to the CERES observations in order to maintain the CERES absolute calibration.

CERES goals include finer time interval averaging steps than monthly means. Daily means and synoptic fields of global fluxes are also planned. This further drives the need for unbiased estimates of broadband flux at times not observed by CERES. The successful incorporation of GEO data with CERES also provides a means of maintaining a stable climate record that is not affected by changes in the temporal sampling from CERES.

This paper presents a description of soon-to-be released CERES monthly mean and shorter time scale products. A detailed description of the methods used to incorporate GEO data into the CERES time record is provided. Broadband estimates from GEO are shown to produce unbiased results relative to CERES as a function of angle and cloud properties. The effectiveness of using GEO to eliminate temporal sampling errors from CERES is shown using comparisons with CERES observations from multiple CERES instruments,

2. CERES MONTHLY PRODUCTS

The CERES Project operationally produces several complementary monthly mean products. For each month of CERES data, the first publicly available time-averaged product is the ERBE-like ES-9 which is designed to provide a climate data record consistent with the Earth Radiation Budget Experiment (ERBE). The second generation CERES monthly mean products, called the Monthly TOA/Surface Averages (SRBAVG), are processed using algorithms that remove angular and sampling biases found in the ERBE-like data and provide additional cloud and radiation information.

The SRBAVG data product contains monthly and monthly-hourly regional, zonal, and global averages of the TOA and surface LW, SW and Window (WN) fluxes along with corresponding cloud properties. The regional means for each 1° equal-angle grid box are calculated by first interpolating each parameter between the times of the CERES observations in order to produce a

*_Corresponding author address_: David F. Young, MS 420, NASA Langley Research Center, Hampton, VA 23681. email: Davd.F.Young@nasa.gov.

complete 1-hourly time series for the month. After interpolation, the time series is used to produce mean parameters on two time scales. Monthly means are calculated using the combination of observed and interpolated parameters from all days containing at least one CERES observation. Monthly-hourly means are produced from the time series by dividing the data into 24 local hour bins to define a monthly mean diurnal cycle. There is one SRBAVG product for each month of data from each CERES instrument. There is also a separate SRBAVG for each possible combination of data from multiple CERES instruments.

SRBAVG products are currently available at the Atmospheric Sciences Data Center (ASDC) (http://eosweb.larc.nasa.gov/) for the CERES Tropical Rainfall Measuring Mission (TRMM) time period (January-August 1998 and March 2000). This paper will describe additional algorithmic development that addresses the unique issues of applying GEO data to CERES data from sun-synchronous satellites such as Terra.

3. METHODOLOGY

Two methods of interpolation are used to produce two separate sets of monthly means that are archived on the SRBAVG. The first interpolation method interpolates the CERES observations using the assumption of constant meteorological conditions similar to the process used to average CERES ERBE-like data. This technique provides the user with monthly fluxes that are more readily compared with the ERBE-like fluxes. These fluxes represent an improvement to ERBE-like fluxes due to improvements to input fluxes, scene identification, and new models of the solar zenith angle dependence of albedo as a function of the CERES ADM scene types (Loeb et al., 2002). The second interpolation method uses 3-hourly 0.65 and 11 μm radiance and cloud property GEO to more accurately model meteorological variability between CERES observations. The GEO data from each satellite are calibrated against coincident Terra Moderate-Resolution Imaging Spectroradiometer (MODIS) imager measurements each month using the technique of Minnis et al. 2002. During the first two years of Terra operations, there were 5 GEO imagers available (Meteosat-5, Meteosat-7, GMS-5, GOES-8, and GOES-10) that provide full longitudinal coverage from 50N – 50S. In order to ensure consistency with CERES cloud products, cloud properties are derived from the GEO data using a subset of the CERES cloud property retrieval algorithms (Minnis et al., 1995). The narrowband radiances are converted to simulated broadband radiances using scene dependent conversions based on matched Visible Infrared Scanner (VIRS) and CERES data. Broadband fluxes are then derived using the CERES TRMM ADM. The TRMM models are used instead of Terra since the TRMM orbit provides more compatible angular sampling relative to the GEO imagers than the sun-synchronous Terra satellite. Finally, the imager-derived flux time series is normalized to the CERES observations to eliminate possible biases due to the limited accuracy of simulating broadband fluxes from narrowband data.

Particular emphasis has been made to create unbiased estimates of broadband flux from the narrowband GEO data. For the LW, TOA flux random errors are 3-5%. It has been demonstrated that 5% biases in LW flux estimates are removed through the normalization process (Young et al. 2002). The SW estimates are much more difficult and subject to errors. These include calibration, ADM, and spectral correction errors. In order for the normalization to accurately account for diurnal changes, it must be demonstrated that the SW flux estimates from GEO are not biased with respect to changing solar zenith angle (SZA) and cloud property changes. A detailed account of the techniques for developing and testing the SW narrowband to broadband (NB-BB) models follows.

4. SW NB-BB MODEL

The NB-BB SW radiance model is a function of viewing and solar geometry, surface type, imager channel, cloud amount, phase and optical depth. The model has been developed using CERES (Wielicki et al. 1998) Single Scanner Footprint (SSF) broadband and VIRS or MODIS imager radiance measurements The radiances were binned similar to the CERES-TRMM ADM (Loeb et al. 2003a). The CERES and imager radiances have the same viewing geometry while the CERES instrument is in the cross-track mode. Measurements were taken during January until August 1998 and March 2000 until February 2002 for the VIRS and MODIS narrowband to broadband models, respectively. The viewing and solar zenith angles were divided into 10° bins and the azimuth angle every 20° except for the first forward and backward scattering bin, which were retained at 10°. The cloudy radiances are separately averaged for water or ice particle clouds. The cloud amount boundaries are 0.1, 15, 50, 85, 99.9, and 100%. The cloud optical depth boundaries are 0.1, 2.5, 6, 10, 18, 40 and 400. The surface types are divided into ocean, forest, grass, dark and bright deserts. Clear-sky albedo thresholds determined the surface types.

Figure 1 shows the VIRS narrowband and CERES broadband reflectance for 3 representative angular bins. There is a strong linear correlation in each of the three cases. The correction between narrowband to broadband is a function of the narrowband reflectance The linear relationships are similar to those found in Trishchenko and Li 1998. Estimating the broadband flux using a linear relationship instead of using a single ratio mitigates the consequences of miss-identified cloud properties. For each bin the following parameters are computed, mean broadband and narrowband reflectance, ratio of the narrowband and broadband reflectance, squared correlation coefficient (r^2), slope and offset of the linear regression. These parameters are shown in Figure 2 for sample clear-sky ocean bins. For clear-sky ocean there is significant angular dependence in the narrowband to broadband reflectances, which needs to be taken into account.

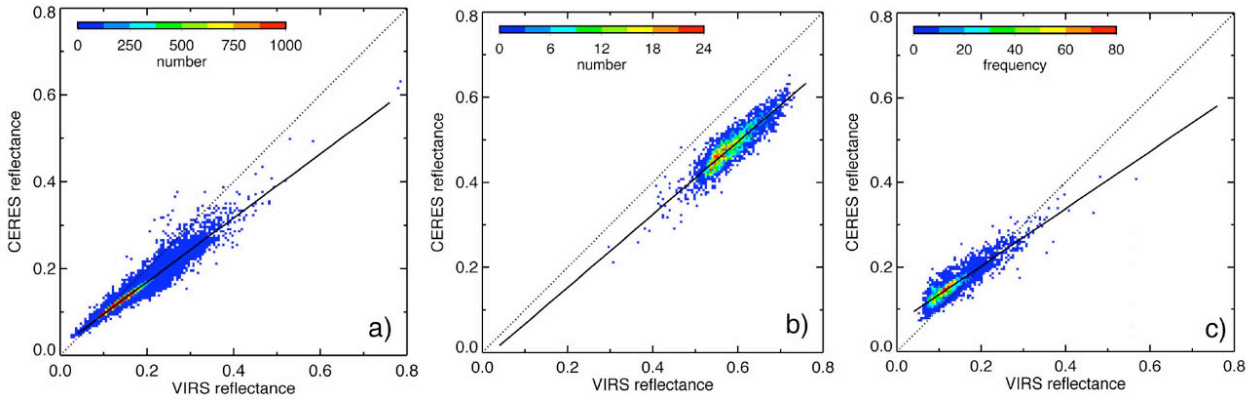

Figure1. a) A scatter plot (color coded by density) of VIRS reflectances and CERES-TRMM SSF reflectances for a clear-sky ocean (glint) bin for the following angles, 35° viewing zenith angle, 20° relative azimuth angle, 35° solar zenith angle, Fig 1b) for a overcast water cloud for optical depths between 18 and 40, and for angles 25°, 60° and 45°. Fig. 1c) for clear-sky grass-land bin for angles 45°, 5° and 55°.

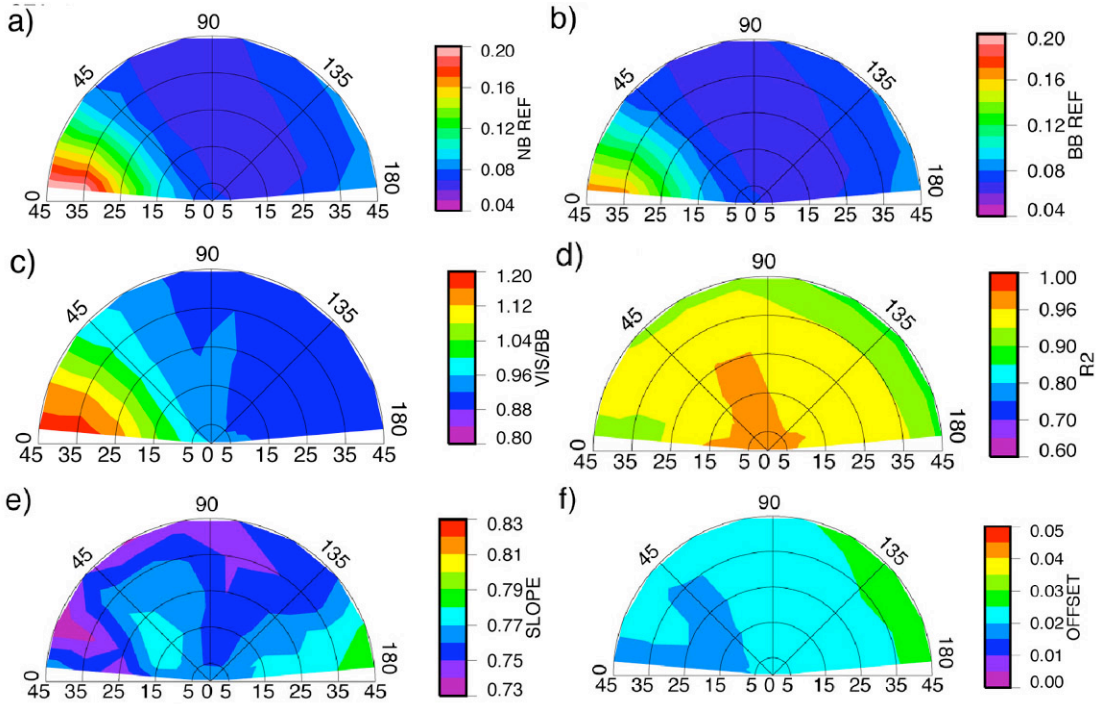

Figure 2a) VIRS angular binned reflectances over clear-ocean for 35° solar zenith angle. The view angle is given on bottom in degrees and the relative azimuth angle is given radially across the top in degrees (forward scatter=0°). Fig. 2b) The corresponding CERES reflectances. Fig. 3c) The ratio of the VIRS and CERES coincident reflectances. Fig 2d) The correlation coefficient of the linear regression of the VIRS and CERES reflectances. Fig. 2c) The slope of the regression. Fig. 2f) The offset of the regression.

A complete set of NB-BB models that includes all possible combinations of angles and scene types cannot be produced due to orbital and scan angle constraints. Since the GEO data are viewed at angles that are not viewed by TRMM or Terra, a method has been developed to extend the observed NB-BB models to unobserved angular bins. Missing bin reflectances are approximated with the use of reflectances from sampled view and azimuth angle bins for given solar zenith, geo and cloud type. A theoretical ratio between an un-sampled and sampled bin reflectances is applied to the observed sampled binned reflectances to estimate the un-sampled reflectances. The details of the theoretical model are described in the next paragraph. The same result can be achieved, to greatly simplify the process, by generating a set number (1000 in this study) of sampled binned narrowband reflectances based on a Gaussian distribution of the mean and standard deviation of the observed narrowband reflectances. The corresponding broadband reflectances are based on the

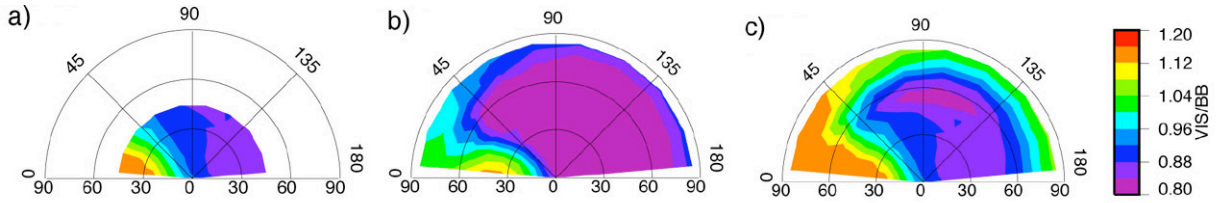

Figure 3a) The ratio of the VIRS and CERES reflectances over clear ocean and solar zenith angle of 35°. The view angle is given on bottom in degrees and the relative azimuth angle is given radially across the top in degrees (forward scatter=0°). Fig. 3b) The ratio of the theoretical narrowband and broadband reflectances. Fig 3c) The combined observed and theoretical ratios.

slope and offset for the given bin. The un-sampled bin is filled with generated narrowband and broadband reflectances after applying the theoretical ratio. This technique essentially normalizes the theoretical reflectances to the observed and maintains the scattering features of the theoretical model. A linear regression is computed for the generated reflectances for each of the un-sampled bins. Figure 3 shows the ratio of narrowband and broadband reflectances for VIRS, theory and the combination of VIRS and theory for clear-sky ocean. The VIRS scanner is limited to 47° view angle. Note the features of the theoretical model (Fig. 3b) are preserved but the magnitude of the ratio is dictated by observations (Fig. 3a) in Fig. 3c.

The theoretical shortwave spectral reflectances are generated using DISORT (Stamnes et al. 1988) for the scattering properties and a correlated k-distribution (Kato et al. 1999) to take into account H2O, CO2, O2, and O3 absorption. A 12 stream (Nakajima and Tanaka 1988) approximation to resolve scattering properties is used to increase efficiency. The shortwave spectrum (0.3-5μm) is divided into 32 bands and 150 sub-bands. The bands are summed to estimate the broadband reflectance. The satellite specific narrowband reflectances were derived by weighting the bands by the spectral response functions (Figure 4). Water clouds are placed between 1 and 3 km and ice cloud between 5 and 7 km into the standard McClatchey mid-latitude summer profile. Water cloud microphysics is based on Mie theory. Ice cloud phase functions are from Yang et al. 2000 and the distributions are from Baum et al. 2000. The 6S ocean surface bidirectional model (Vermote et al. 1997) and prairie and desert bidirectional properties from Ahmad and Deering 1992 are used. A clear-sky aerosol optical depth of 0.2 was used. Partial cloudy reflectances are computed by linearly weighting the contributions of the clear and overcast reflectances.

Figure 5 shows the albedos as a function solar zenith angle for various surface types and optically thick ice and water clouds The cloudy cases in Fig. 5 have no surface contribution and have an optical depth of 27.5. As Raleigh scattering increases as a function of solar zenith angle the narrowband to broadband converges to unity. The ocean albedo is the mean of narrowband to broadband ratios of 0.8 in the non-glint to 1.2 in the glint angles. Over vegetation the near IR reflectance is not measured in the VIRS visible channel thereby reducing the ratio as low as 0.65 and 0.9 for forest and grass, respectively. For deserts this is the global ratio, since each desert has its own spectral signal.

In order to incorporate various geostationary visible bands into the narrowband to broadband model, theoretical Meteosat-7 and 5, GMS-5, and GOES-10 and 8 reflectances are computed for the same bins as the narrowband to broadband model. For a given set of angles, surface type, cloud amount and phase, six optical depth bins and one clear-sky VIRS and geostationary reflectances are available The reflectance sequence from clear-sky to optically thick cloud (no surface contribution) provides the basis for performing a linear regression between the VIRS and geostationary

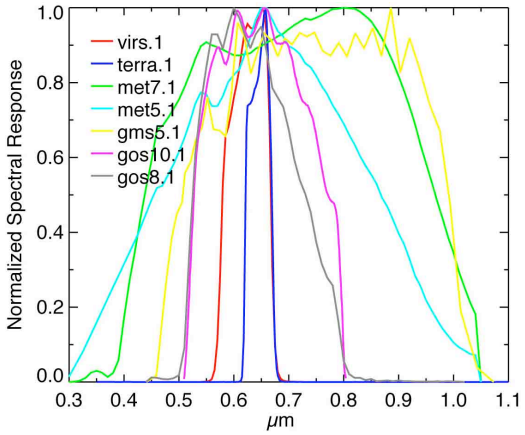

Figure 4 Plot of the geostationary, VIRS and MODIS imager spectral response functions.

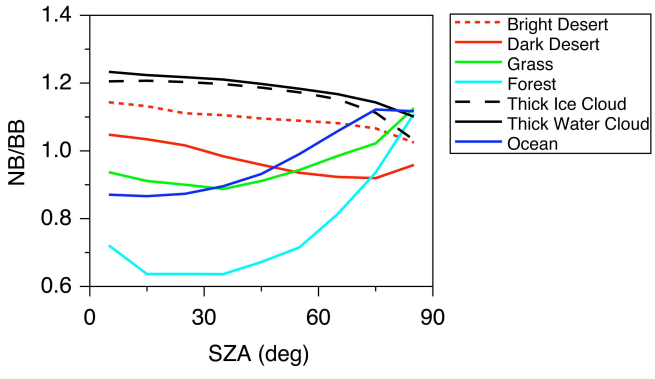

Figure 5 Plot of the ratio of the VIRS and CERES albedos for various scene types as a function of solar zenith angle.

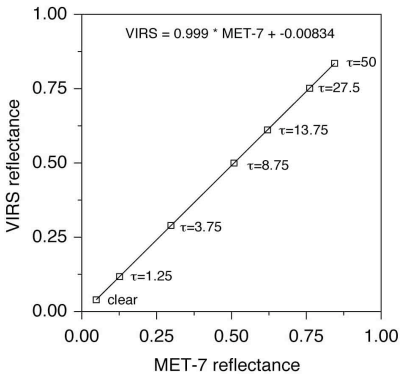

Figure 6. A scatter plot of the theoretical Meteosat-7 and VIRS reflectances of various optical depths for an overcast ice cloud at a 35° solar zenith angle, an 90° azimuth angle and a 35° viewing angle. The corresponding slope and offset of the linear regression is given at the top.

reflectances (Figure 6). For a given geostationary reflectance, the reflectance is adjusted to an equivalent VIRS reflectance using the linear regression coefficients and then the narrowband to broadband model is applied.

5. RESULTS

The NB-BB model can be tested for consistency using CERES- Rotating Azimuth Plane Scan (RAPS) SSF data. In RAPS mode the VIRS scan pattern is in cross-track mode but the CERES instrument rotates azimuthally. In RAPS mode the view and relative azimuth angles are different for the narrowband and broadband reflectances but the solar zenith angle remains constant. The narrowband to broadband model

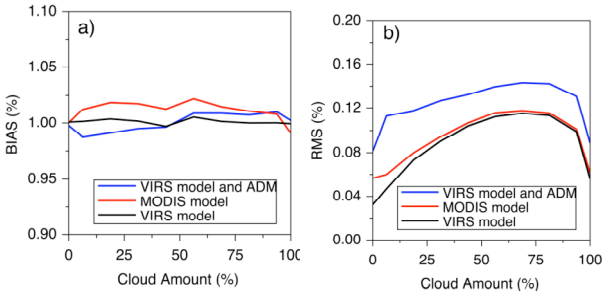

Figure 7a) The black line is the ratio (bias) of the VIRS derived and CERES-SSF broadband ocean reflectances using the NB-BB model as a function of cloud amount. The blue line also applies the CERES ADM to the VIRS derived broadband reflectances and the ratio of the VIRS derived broadband and CERES flux is shown. The red line represents the VIRS derived broadband reflectances using the MODIS narrowband to broadband model after adjusting the VIRS reflectance to an equivalent MODIS reflectance. Figure 7b) Same as Fig. 7a) except for rms error.

is applied to the VIRS reflectances and then the CERES-TRMM ADM converts the VIRS derived broadband reflectances into fluxes. These fluxes can be compared to the CERES fluxes. To validate the narrowband adjustment algorithm the VIRS reflectances are converted toMODIS equivalent reflectances and the MODIS to broadband reflectance model is applied. Figure 7 shows these results using every fourth day of the 1998 dataset. The biases (Figure 6a) are within 3% as a function of cloud amount. The VIRS model bias should be close to unity, since the narrowband to broadband model was based on that same dataset. The VIRS to MODIS adjustment appears to work well in cloudy conditions, since the rms error is nearly the same whether using the MODIS or VIRS model. Over clear-sky conditions some error is introduced. The predicted broadband flux rms errors are as low as 8% for overcast and clear-sky conditions and as a high as 14% for partly cloudy conditions with no functionality with solar zenith angle in either the bias or rms error.

The flatness of the biases in estimated SW flux with respect to cloud fraction and SZA is of particular importance when applying the GEO correction to sun-synchronous data such as from Terra. SW data from Terra is

The interpolated GEO fluxes can be tested directly using a combination of Aqua and Terra data. Morning observations from Terra can be interpolated to the afternoon observation times of Aqua to estimate interpolation errors. Without GEO data, monthly zonal mean fluxes from Aqua and Terra can differ by up to 10 W/m2 in the SW and 4 W/m2 in the LW. Figure 8 shows the time series of Aqua-Terra zonal mean ERBE-like TOA flux differences over the period July 2002-June 2003. Note the large differences in the Southern Hemisphere where the time difference between Aqua and Terra is maximized.

This difference is not unique to the ERBE-like product. The non-GEO SRBAVG monthly means will produce a similar result due to the assumption of

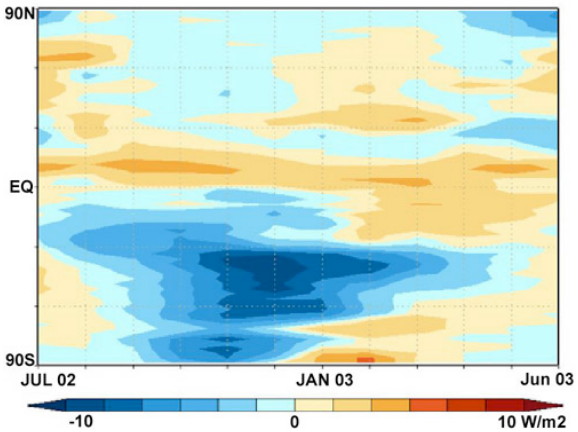

Figure 8. Time Series of ERBElike Aqua-Terra monthly zonal mean TOA SW flux differences. Blue regions represent monthly mean fluxes from Terra are greater than Aqua.

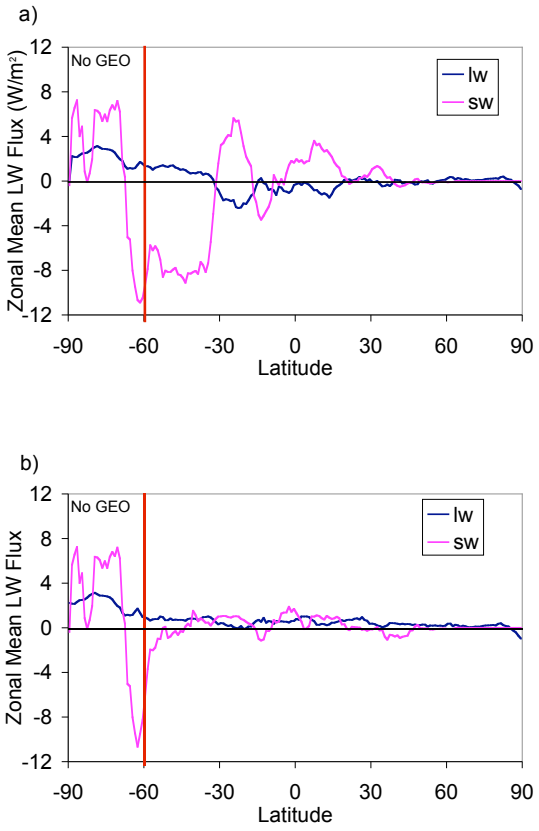

Figure 9. monthly-zonal mean Aqua-Terra differences in SW and LW TOA flux from SRBAVG. Figure 9a shows the non-GEO differences while 9b shows the improvement from adding GEO data to the interpolation process.

constant meteorology in the interpolation process. The zonal mean differences from a Beta version of the SRBAVG product is shown for December 2002 in Figure 9a. Once again, zonal mean TOA SW flux differences exceed 8 W/m2 between 30S and 65S. The introduction of GEO data removes the major biases as shown in Figure 9b. Both LW and SW zonal mean flux differences are reduced to less than 2 W/m2 at all latitudes where GEO data are available. Polar latitudes are unaffected since there is no additional data. Flux estimates for these regions will be greatly improved by a combined Aqua/Terra product. The first 3 years of CERES Terra SRBAVG products are scheduled to be archived and made publicly available at the ASDC in fall 2004.

6. FUTURE WORK

Testing of the NB-BB models and their implementation into the CERES interpolation process continues. Flux estimation accuracy is being assessed for the first 3 years of Terra data as a function of sza, cloud fraction, GEO satellite, and month. Currently the best test of these data is the Terra/Aqua comparison, but future tests will be performed with broadband surface flux time series. Finally, the best test of the TOA flux interpolation process will be comparisons against the GERB data once validation of that data set is completed.

REFERENCES

Ahmad, S. P., D. W. Deering, 1992: A simple analytical function for bidirectional reflectance, *J. Geophys. Res.*, **97**, 18867-18886.

Baum, B. A., P. Yang, S. C. Ou, Y. Hu, P. F. Soulen, S.-C. Tsay, 2000: Remote sensing of cloud properties using MODIS airborne simulator imagery during SUCCESS.Part I: Data and models, *J. Geophys. Res.*, **105**, 11767-11780.

Gupta, S. K. D. P. Kratz, P. W. Stackhouse, Jr. and A. C. Wilber, 2001: The Langley Parameterized Shortwave Algorithm (LPSA) for Surface Radiation Budget Studies, NASA TP 2002-211272, 31 pp.

Gupta, Shashi K., Kratz, David P., Wilber, Anne C., Nguyen, L. Cathy. 2004: Validation of Parameterized Algorithms Used to Derive TRMM–CERES Surface Radiative Fluxes. *Journal of Atmospheric and Oceanic Technology*: Vol. 21, No. 5, pp. 742–752.

Kato, S, T. P. Ackerman, J. H. Mather, and E. E. Clothiaux, 1999: The k-distribution method and correlated-k approximation for a shortwave radiative transfer model. *J. Quant. Spectrosc. Radiat. Transfer*, **62**, 109-121.

Loeb, Norman G., Manalo-Smith, Natividad, Kato, Seiji, Miller, Walter F., Gupta, Shashi K., Minnis, Patrick, Wielicki, Bruce A. 2003a: Angular Distribution Models for Top-of-Atmosphere Radiative Flux Estimation from the Clouds and the Earth's Radiant Energy System Instrument on the Tropical Rainfall Measuring Mission Satellite. Part I: Methodology. *Journal of Applied Meteorology*: Vol. 42, No. 2, pp. 240–265.

Loeb, Norman G., Loukachine, Konstantin, Manalo-Smith, Natividad, Wielicki, Bruce A., Young, David F. 2003b: Angular Distribution Models for Top-of-Atmosphere Radiative Flux Estimation from the Clouds and the Earth's Radiant Energy System Instrument on the Tropical Rainfall Measuring Mission Satellite. Part II: Validation. *Journal of Applied Meteorology*: Vol. 42, No. 12, pp. 1748–1769.

Minnis, P. et al., 1995: Cloud Optical Property Retrieval (Subsystem 4.3). In *Clouds and the Earth's Radiant Energy System (CERES) Algorithm Theoretical Basis Document, Volume III: Cloud Analyses and Radiance Inversions (Subsystem 4)*, *NASA RP 1376 Vol. 3*, edited by CERES Science Team, pp. 135-176.

Minnis, P., L. Nguyen, D. R. Doelling, D. F. Young, W. F. Miller, and D. P. Kratz, 2002: Rapid calibration of operational and research meteorological satellite imagers. Part I and II. *J. Atmos. Oceanic Technol.*, in press.

Nakajima, T. M. Tanaka, 1988: Algorithms for radiative intensity calculations in moderately thick

atmospheres using a truncation approximation, *J. Quant. Spectrosc. Radiant. Transfer*, **40**, 51-69.

Stamnes, K., S-C. Tsay, W. Wiscombe, and K. Jayaweera, 1988: Numerically stable algorithm for discrete-ordinate-method radiative transfer in multiple scattering and emitting layered media, *Appl. Opt*., **27**, 2502-2509.

Standfuss, Carsten, Viollier, Michel, Kandel, Robert S., Duvel, Jean Philippe, 2001: Regional Diurnal Albedo Climatology and Diurnal Time Extrapolation of Reflected Solar Flux Observations: Application to the ScaRaB Record. *Journal of Climate*: Vol. 14, No. 6, pp. 1129–1146.

Trishchenko, A, and Z Li, 1998: Use of ScaRAB Measurements for Validating a GOES-Based TOA Radiation Product, *J. Applied Meteor.* **37**, 591-605.

Vermote, E. F., Tanre, D., Morcrette, J.-J., 1997: Second Simulation of the Satellite Signal in the Solar Spectrum, 6S: An Overview. *IEEE transactions on geoscience and remote sensing*, **35**, 675-686.

Viollier M., R. Kandel, P. Raberanto, 2004, Combination of ScaRaB-2 and CERES with Meteosat-5 to remove time sampling bias and improve radiation budget estimations in the INDOEX region, J. Geophys. Res., 109, D05105, doi:10.1029/2003JD003947.

Wielicki, B. A., B. R. Barkstrom, E. F. Harrison, R. B. Lee III, G. L. Smith, and J. E. Cooper, 1996: Clouds and the Earth's Radiant Energy System (CERES): An Earth Observing System Experiment. *Bull. Amer. Meteor. Soc*., **77**, 853-868.

Wielicki, B. A., B. R. Barkstrom, B. A. Baum, T. P. Charlock, R. N. Green, D. P. Kratz, R. B. Lee, P. Minnis, G. L. Smith, D. F. Young, R. D. Cess, J. A. Coakley, D. Crommelynck, L. Donner, R. Kandel, M. D. King, A. J. Miller, V. Ramanathan, D. A. Randall, L. L. Stowe, and R. M. Welch, 1998: Clouds and the Earth's Radiant Energy System (CERES): Algorithm overview. *IEEE Trans. Geosci. Remote Sens.*, **36**, 1127-1141.

Yang, P., K.-N. Liou, K. Wyser, and D. Mitchell, 2000:Parameterization of the scattering and absorption properties of individual ice crystals, *J. Geophys. Res*., **105**, 4699-4718.

Young, D. F., P. Minnis, D. R. Doelling, G. G. Gibson, and T. Wong, 1998: Temporal Interpolation Methods for the Clouds and Earth's Radiant Energy System (CERES) Experiment. *J. Appl. Meteorol.,* **37**, 572-590.

Young, D. F., B. A. Wielicki, T. Wong, M. A. Haeffelin, D. R. Doelling, J. D. Kenyon, and J. S. Boghosian, 2002: New Geostationary-enhanced CERES Monthly Mean Radiative Fluxes and Cloud Properties. *Proceedings of the 11th AMS Conference on Atmospheric Radiation*, Ogden, UT, June 3 - June 7.